Inorg. Chem. **2007**, *46*, 4158–4166

Exceptional Self-Penetrating Networks Containing Unprecedented Quintuple-Stranded Molecular Braid, 9-Fold Meso Helices, and 17-Fold Interwoven Helices

Dong-Rong Xiao, Yang-Guang Li, En-Bo Wang,* Lin-Lin Fan, Hai-Yan An, Zhong-Min Su,* and Lin Xu

Key Laboratory of Polyoxometalate Science of Ministry of Education, Institute of Polyoxometalate Chemistry, Department of Chemistry, Northeast Normal University, Changchun 130024, People's Republic of China

Received January 11, 2007

Self-assembly of long V-shaped ligands and d^{10} metal salts in the presence of a linear bidentate ligand affords two unprecedented self-penetrating coordination networks $\{[Zn_4(bptc)_2(bpy)_4]\cdot(C_5H_3N)\cdot 4H_2O\}_n$ (**1**) and $\{[Cd_2(sdba)_2(bpy)(H_2O)_2]\cdot 2H_2O\}_n$ (**2**) (bptc = 3,3′,4,4′-benzophenonetetracarboxylate, sdba = 4,4′-sulfonyldibenzoate, bpy = 4,4′-bipyridine). Their structures were determined by single-crystal X-ray diffraction analyses and further characterized by elemental analyses, IR spectra, X-ray powder diffraction, and TG analyses. **1** adopts a novel 3D framework containing three types of molecular braids, among which the quintuple-stranded molecular braid represents the highest-stranded molecular braid presently known for entangled systems. **2** is an uncommon self-penetrating 2D network containing pseudo-Borromean links and double-stranded helices. More interestingly, when the strong hydrogen bonds between layers are taken into account, the resulting net of **2** becomes an eight-connected 3D self-penetrating network with an unprecedented ($4^{21}.6^7$) topology, which represents the highest connected topology presently known in self-penetrating systems. Furthermore, the photoluminescent properties of **1** and **2** were studied.

Introduction

Crystal engineering of metal−organic frameworks (MOFs) is of great current interest not only because of its tremendous potential applications in gas storage, chemical separations, microelectronics, nonlinear optics, and heterogeneous catalysis, but also because of its intriguing structural diversity, new topologies, and intricate entangled motifs.[1] Entangled systems, one of the major themes of supramolecular chemistry, are common in biology (as seen in catenanes, rotaxanes, and molecular knots) and have attracted a great deal of attention from chemists because of their intrinsic aesthetic appeal[2], and more importantly, because of their interesting properties and potential applications ranging from drug delivery vehicles to sensor devices.[3] Interpenetrating networks, which have been the most investigated type of entanglement, can be described as polymeric analogues of catenanes and rotaxanes.[5] They have provided a long-standing fascination for chemists, and many appealing interpenetrated frameworks have been constructed[4] and discussed in comprehensive reviews by Batten and Robson.[5]

* To whom correspondence should be addressed. E-mail: wangenbo@public.cc.jl.cn. Fax: +86-431-85098787.

(1) (a) Moulton, B.; Zaworotko, M. J. *Chem. Rev.* **2001**, *101*, 1629. (b) Evans, O. R.; Lin, W. *Acc. Chem. Res.* **2002**, *35*, 511. (c) Janiak, C. *J. Chem. Soc., Dalton Trans*. **2003**, 2781. (d) Kitagawa, S.; Kitaura, R.; Noro, S. I. *Angew. Chem., Int. Ed.* **2004**, *43*, 2334. (e) Rao, C. N. R.; Natarajan, S.; Vaidhyanathan, R. *Angew. Chem., Int. Ed.* **2004**, *43*, 1466. (f) Ockwig, N. W.; Delgado-Friederichs, O.; O'Keeffee, M.; Yaghi, O. M. *Acc. Chem. Res*. **2005**, *38*, 176. (g) Yaghi, O. M.; O'Keeffe, M.; Ockwig, N. W.; Chae, H. K.; Eddaoudi, M.; Kim, J. *Nature*. **2003**, *423*, 705.

(2) (a) Carlucci, L.; Ciani, G.; Proserpio, D. M. *Coord. Chem. Rev*. **2003**, *246*, 247. (b) Carlucci, L.; Ciani, G.; Proserpio, D. M. *CrystEngComm.* **2003**, *5*, 269. (c) Bourne, S. A.; Lu, J.; Moulton, B.; Zaworotko, M. J. *Chem. Commun.* **2001**, 861. (d) Bu, X. H.; Tong, M. L.; Chang, H. C.; Kitagawa, S.; Batten, S. R. *Angew. Chem., Int. Ed.* **2004**, *43*, 192.

(3) (a) Sauvage, J. P. *Acc. Chem. Res*. **1998**, *31*, 611. (b) Kim, K. *Chem. Soc. Rev*. **2002**, *31*, 96. (c) Fujita, M.; Sasaki, O.; Watanabe, K.; Ogura, K.; Yamaguchi, K. *New. J. Chem.* **1998**, *22*, 189. (d) Carlucci, L.; Ciani, G.; Moret, M.; Proserpio, D. M.; Rizzato, S. *Angew. Chem., Int. Ed.* **2000**, *39*, 1506.

(4) (a) Blatov, V. A.; Carlucci, L.; Ciani, G.; Proserpio, D. M. *CrystEngComm* **2004**, *6*, 377. (b) Liang, K.; Zheng, H.; Song, Y.; Lappert, M. F.; Li, Y.; Xin, X.; Huang, Z.; Chen, J.; Lu, S. *Angew. Chem., Int. Ed.* **2004**, *43*, 5776. (c) Park, K. M.; Whang, D.; Lee, E.; Heo, J.; Kim, K. *Chem.—Eur. J.* **2002**, *8*, 498. (d) Niel, V.; Thompson, A. L.; Muñoz, M. C.; Galet, A.; Goeta, A. E.; Real, J. A. *Angew. Chem., Int. Ed.* **2003**, *42*, 3760. (e) Aitken, J. A.; Kanatzidis, M. G. *J. Am. Chem. Soc.* **2004**, *126*, 11780.

(5) (a) Batten, S. R.; Robson, R. *Angew. Chem., Int. Ed.* **1998**, *37*, 1460. (b) Batten, S. R. *CrystEngComm* **2001**, *3*, 67.

10.1021/ic070054a CCC: $37.00
Published on Web 04/21/2007

However, the study of self-penetrating (polyknotting) networks considered as polymeric equivalents of molecular knots remains largely unexplored, as evidenced in a recent review by Ciani and co-workers.[2a] According to Robson, Ciani, Champness, and their co-workers,[2a,6] self-penetration is a single net having the peculiarity that the smallest topological rings are catenated by other smallest rings belonging to the same net. In contrast to the fruitful production of interpenetrating networks, the self-penetration feature is still uncommon within coordination polymers, and only a few elegant examples belonging to this family have been reported so far,[6] implying a new challenging issue in coordination chemistry.

On the other hand, particular attention has recently been devoted to the finding of frames with novel entanglements, such as multiple helices, Borromean architectures, and polyrotaxanes,[2] that contribute to increasing our knowledge of the self-assembly processes.[6g,8] Multiple helices, which are ubiquitous in nature and are the foundation of genetic codes, are attracting increased attention in coordination chemistry and material chemistry originating from their importance in biological systems, optical devices, and asymmetric catalysis.[1a,7] Driven by the pioneering work of Lehn and co-workers,[8] some appealing coordination polymers containing multiple helices have been constructed.[9] In contrast, the occurrence of multiple meso helices (hereafter referred to as molecular braid[10]) is surprisingly rare, although meso helices are often found in nature and in everyday use, as known for tendrils of a variety of plants, hair braids, and telephone wires.[11] To the best of our knowledge, only two fascinating triple-stranded molecular braids have been characterized up to now, both constructed from three interwoven single-stranded meso helices.[10] However, no higher-stranded molecular braids have been reported hitherto. Therefore, the construction of higher-stranded molecular braids is still a formidable challenge for synthetic chemists, and further research is necessary to enrich and develop this branch. Herein, during the course of our attempts to synthesize novel entangled networks,[12] we report two intriguing self-penetrating nets, namely, $\{[Zn_4(bptc)_2(bpy)_4]\cdot(C_5H_3N)\cdot 4H_2O\}_n$ (**1**) and $\{[Cd_2(sdba)_2(bpy)(H_2O)_2]\cdot 2H_2O\}_n$ (**2**) (bptc = 3,3′,4,4′-benzophenonetetracarboxylate (Scheme 1), sdba = 4,4′-sulfonyldibenzoate (Scheme 2), bpy = 4,4′-bipyridine), both exhibiting unprecedented topologies. **1** and **2** have several unusual features: (1) The 3D framework of **1** contains three types of molecular braids, among which the quintuple-

Scheme 1 [a]

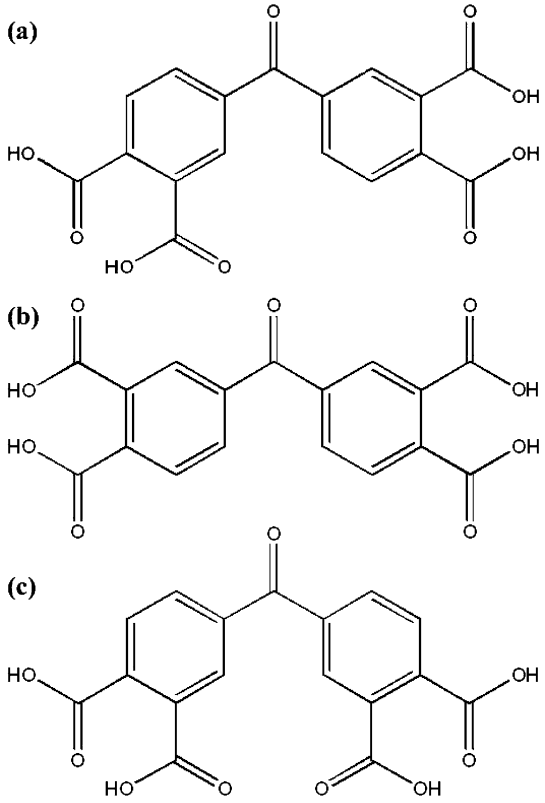

[a] Three possible conformations of H_4bptc. The conformation in **1** is shown in (c).

(6) (a) Abrahams, B. F.; Hardie, M. J.; Hoskins, B. F.; Robson, R.; Sutherland, E. E. *Chem. Commun.* **1994**, 1049. (b) Carlucci, L.; Ciani, G.; Proserpio, D. M.; Porta, F. *Angew. Chem., Int. Ed.* **2003**, *42*, 317. (c) Jensen, P.; Price, D. J.; Batten, S. R.; Moubaraki, B.; Murray, K. S. *Chem.—Eur. J.* **2000**, *6*, 3186. (d) Abrahams, B. F.; Batten, S. R.; Grannas, M. J.; Hamit, H.; Hoskins, B. F.; Robson, R. *Angew. Chem., Int. Ed.* **1999**, *38*, 1475. (e) Withersby, M. A.; Blake, A. J.; Champness, N. R.; Cooke, P. A.; Hubberstey, P.; Schröder, M. *J. Am. Chem. Soc.* **2000**, *122*, 4044. (f) Tong, M. L.; Chen, X. M.; Batten, S. R. *J. Am. Chem. Soc.* **2003**, *125*, 16170. (g) Carlucci, L.; Ciani, G.; Proserpio, D. M.; Rizzato, S. *J. Chem. Soc., Dalton Trans.* **2000**, 3821. (h) Long, D. L.; Hill, R. J.; Blake, A. J.; Champness, N. R.; Hubberstey, P.; Wilson, C.; Schröder, M. *Chem.—Eur. J.* **2005**, *11*, 1384.

(7) (a) Nakano, T.; Okamoto, Y. *Chem. Rev.* **2001**, *101*, 4013. (b) Albrecht, M. *Chem. Rev.* **2001**, *101*, 3457. (c) Soghomonian, V.; Chen, Q.; Haushalter, R. C.; Zubieta, J.; O'Connor, C. J. *Science* **1993**, *259*, 1596. (d) Song, Y.; Yu, J.; Li, Y.; Li, G.; Xu, R. *Angew. Chem., Int. Ed.* **2004**, *43*, 2399. (e) Han, L.; Hong, M. C. *Inorg. Chem. Commun.* **2005**, *8*, 406.

(8) (a) Lehn, J.-M.; Rigault, A.; Siegel, J.; Harrowfield, J.; Chevrier, B.; Moras, D. *Proc. Natl. Acad. Sci. U.S.A.* **1987**, *84*, 2565. (b) Berl, V.; Huc, I.; Khoury, R. G.; Krische, M. J.; Lehn, J.-M. *Nature* **2000**, *407*, 720. (c) Lehn, J.-M. *Supramolecular Chemistry;* VCH: Weinheim, Germany, 1995.

(9) (a) Cui, Y.; Lee, S. J.; Lin, W. *J. Am. Chem. Soc.* **2003**, *125*, 6014. (b) Chen, X. M.; Liu, G. F. *Chem.—Eur. J.* **2002**, *8*, 4811. (c) Bau, R. *J. Am. Chem. Soc.* **1998**, *120*, 9380. (d) Jouaiti, A.; Hosseini, M.W.; Kyritsakas, N. *Chem. Commun.* **2003**, 472. (e) Grosshansa, P.; Jouaitia, A.; Bulacha, V.; Planeixa, J.-M.; Hosseini, M.W.; Nicoudb, J.-F. *Chem. Commun.* **2003**, 1336. (f) Xiao, D. R.; Wang, E. B.; An, H. Y.; Li, Y. G.; Su, Z. M.; Sun, C. Y. *Chem.—Eur. J.* **2006**, *12*, 6528.

(10) (a) Luan, X.-J.; Wang, Y.-Y.; Li, D.-S.; Liu, P.; Hu, H.-M.; Shi, Q.-Z.; Peng, S.-M. *Angew. Chem., Int. Ed.* **2005**, *44*, 3864. (b) Luan, X.-J.; Cai, X.-H.; Wang, Y.-Y.; Li, D.-S.; Wang, C.-J.; Liu, P.; Hu, H.-M.; Shi, Q.-Z.; Peng, S.-M. *Chem.—Eur. J.* **2006**, *12*, 6281.

(11) (a) Plasseraud, L.; Maid, H.; Hampel, F.; Saalfrank, R. W. *Chem.—Eur. J.* **2001**, *7*, 4007. (b) Becker, G.; Eschbach, B.; Mundt, O.; Seidler, N. *Z. Anorg. Allg. Chem.* **1994**, *620*, 1381. (c) Bartlett, R. A.; Olmstead, M. M.; Power, P. P. *Inorg. Chem.* **1986**, *25*, 1243.

(12) (a) Wang, X. L.; Qin, C.; Wang, E. B.; Xu, L.; Su, Z. M.; Hu, C. W. *Angew. Chem., Int. Ed.* **2004**, *43*, 5036. (b) Wang, X. L.; Qin, C.; Wang, E. B.; Li, Y. G.; Su, Z. M.; Xu, L.; Carlucci, L. *Angew. Chem., Int. Ed.* **2005**, *44*, 5824. (c) Qin, C.; Wang, X. L.; Carlucci, L.; Tong, M. L.; Wang, E. B.; Hu, C. W.; Xu, L. *Chem. Commun.* **2004**, 1876. (d) Wang, X. L.; Qin, C.; Wang, E. B.; Li, Y. G.; Su, Z. M. *Chem. Commun.* **2005**, 5450. (e) Xiao, D. R.; Wang, E. B.; An, H. Y.; Su, Z. M.; Li, Y. G.; Gao, L.; Sun, C. Y.; Xu, L. *Chem.—Eur. J.* **2005**, *11*, 6673. (f) Wang, X. L.; Qin, C.; Wang, E. B.; Su, Z. M.; Xu, L.; Batten, S. R. *Chem. Commun.* **2005**, 4789. (g) Wang, X. L.; Qin, C.; Wang, E. B.; Su, Z. M. *Chem.—Eur. J.* **2006**, *12*, 2680. (h) Xiao, D. R.; Wang, E. B.; An, H. Y.; Li, Y. G.; Xu, L. *Cryst. Growth Des.* **2007**, *7*, 507.

(13) (a) Carlucci, L.; Ciani, G.; Proserpio, D. M.; Rizzatio, S. *Chem.—Eur. J.* **2002**, *8*, 1520. (b) Carlucci, L.; Ciani, G.; Proserpio, D. M. *Chem. Commun.* **2004**, 380.

Scheme 2 [a]

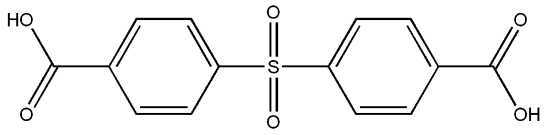

[a] Structure of H_2sdba.

stranded molecular braid represents the highest-stranded molecular braid presently known for entangled systems. (2) The 9-fold interwoven meso helices (found in **1**) constructed from three triple-stranded molecular braids are unprecedented. (3) The structure of **1** consists of the exceptional entangled motifs originated from 17 interwoven helices. (4) **2** is an uncommon self-penetrating 2D network containing pseudo-Borromean links and double-stranded helices. (5) When the strong hydrogen bonds between layers are taken into account, the resulting net of **2** becomes an eight-connected 3D self-penetrating network with an unprecedented ($4^{21}.6^7$) topology, which represents the highest-connected topology presently known in self-penetrating systems.

Experimental Section

General Considerations. All of the chemicals were commercially purchased and used without further purification. Elemental analyses (C, H, and N) were performed on a Perkin-Elmer 2400 CHN Elemental Analyzer. Zn and Cd were determined by a Leaman inductively coupled plasma (ICP) spectrometer. IR spectra were recorded in the range of 400−4000 cm^{-1} on an Alpha Centaurt FT/IR Spectrophotometer using KBr pellets. TG analyses were performed on a Perkin-Elmer TGA7 instrument in flowing N_2 with a heating rate of 10 °C·min^{-1}. Excitation and emission spectra were obtained on a SPEX FL-2T2 spectrofluorometer equipped with a 450 W xenon lamp as the excitation source. XRPD data were recorded on a Siemens D5005 diffractometer using Cu Kα radiation.

Synthesis of $\{[Zn_4(bptc)_2(bpy)_4]\cdot(C_5H_3N)\cdot 4H_2O\}_n$ (1). A mixture of $Zn(NO_3)_2\cdot 6H_2O$ (0.5 mmol), H_4bptc (0.25 mmol), bpy (0.75 mmol), and water (8 mL) was stirred for 30 min in air, then transferred and sealed in an 18 mL Teflon-lined autoclave, which was heated at 150 °C for 3 d (Scheme S3). After slow cooling to room temperature, colorless block crystals of **1** were filtered off, washed with distilled water, and dried in air (yield: 42% based on Zn). The powder X-ray diffraction pattern of the bulk product was in agreement with the simulated pattern from single-crystal analysis, demonstrating the phase purity of the product (Figure S32). Anal. Calcd for $C_{79}H_{55}N_9O_{22}Zn_4$: C, 54.41; H, 3.18; N, 7.23; Zn, 15.00. Found: C, 54.07; H, 3.39; N, 7.52; Zn, 14.74. IR (KBr, cm^{-1}): 3346 (brm), 3115(w), 3067(w), 1658(w), 1609(s), 1590(s), 1574(s), 1487(s), 1407(s), 1368(s), 1304(m), 1261(w), 1247(m), 1224(w), 1177(w), 1135(w), 1063(s), 1041(w), 1015(w), 988(w), 925(w), 913(w), 849(s), 813(m), 799(m), 770(w), 759(m), 721(m), 709(w), 667(w), 638(m), 613(w), 587(w), 569(w), 528(m), 460(w), 409(w).

Synthesis of $\{[Cd_2(sdba)_2(bpy)(H_2O)_2]\cdot 2H_2O\}_n$ (2). A mixture of $Cd(NO_3)_2\cdot 4H_2O$ (0.5 mmol), H_2sdba (0.5 mmol), bpy (0.25 mmol), and water (8 mL) was stirred for 30 min in air, then transferred and sealed in an 18 mL Teflon-lined autoclave, which was heated at 150 °C for 3 d (Scheme S3). After slow cooling to the room temperature, yellow block crystals of **2** were filtered off, washed with distilled water, and dried in air (yield: 66% based on Cd). The powder X-ray diffraction pattern of the bulk product was in agreement with the simulated pattern from single-crystal analysis, demonstrating the phase purity of the product (Figure S33). Anal. Calcd for $C_{38}H_{32}Cd_2N_2O_{16}S_2$: C, 42.99; H, 3.04; Cd, 21.18; N, 2.64. Found: C, 43.31; H, 3.27; Cd, 20.96; N, 2.88. IR (KBr, cm^{-1}): 3541 (s), 3386 (brm), 3100(w), 1825(w), 1612(s), 1592(s), 1539(s), 1490(m), 1405(s), 1323(s), 1296(s), 1221(m), 1166(s), 1133(m), 1102(s), 1068(m), 1016(m), 871(m), 858(s), 815(m), 782(m), 750(s), 729(m), 694(m), 667(w), 637(w), 621(s), 584(m), 521(m), 491(m), 462(m), 426(w).

Table 1. Crystal Data and Structure Refinement for **1** and **2**

complex	**1**	**2**
formula	$C_{79}H_{55}N_9O_{22}Zn_4$	$C_{38}H_{32}Cd_2N_2O_{16}S_2$
fw	1743.80	1061.58
T (K)	293(2)	293(2)
λ (Å)	0.71073	0.71073
cryst syst	monoclinic	monoclinic
space group	$C2/c$	$C2/c$
a (Å)	18.786(4)	19.144(4)
b (Å)	16.768(3)	9.934(2)
c (Å)	12.803(3)	21.129(4)
β (deg)	100.02(3)	100.90(3)
V (Å^3)	3971.6(14)	3945.9(14)
Z	2	4
D_c (g/cm^3)	1.458	1.787
μ (mm^{-1})	1.273	1.261
R1[a] [$I > 2\sigma(I)$]	0.0767	0.0239
wR2[b] [$I > 2\sigma(I)$]	0.1413	0.0688

[a] $R1 = \sum||F_0| - |F_C||/\sum|F_0|$. [b] $wR2 = \sum[w(F_0^2 - F_C^2)^2]/\sum[w(F_0^2)^2]^{1/2}$

X-ray Crystallography. Suitable single crystals with dimensions of 0.51 × 0.42 × 0.38 mm^3 for **1** and 0.54 × 0.51 × 0.47 mm^3 for **2** were glued on a glass fiber. Diffraction intensity data were collected on a Rigaku R-AXIS RAPID IP diffractometer with Mo Kα monochromated radiation ($\lambda = 0.71073$ Å) at 293 K. Empirical absorption correction was applied. The structures were solved by the direct method and refined by the full-matrix least-squares method on F^2 using the SHELXL-97 software.[14] All non-hydrogen atoms were refined anisotropically. The organic hydrogen atoms were generated geometrically. In **1**, the aqua hydrogen atoms were not located. In **2**, exact positions of the hydrogen atoms attached to OW1 and OW2 were located from the difference Fourier maps. The crystal data and structure refinement of **1** and **2** are summarized in Table 1. Selected bond lengths and angles for **1** and **2** are listed in Table 2.

The CCDC reference numbers are 618580 for **1** and 618579 for **2**.

Results and Discussion

Syntheses. Our strategy of employing two long V-shaped ligands, such as bptc and sdba, was based on the following considerations: (i) employment of V-shaped bridging ligands could improve the helicity of the polymeric chains, which may thus favor the formation of helical and meso helical structure.[7−11] (ii) Long flexible ligands have shown the ability to produce unique interwoven motifs because of their varied conformations (Scheme 1) and geometries.[12,13] (iii) Coordination polymers constructed from the bptc ligand are comparatively unexplored. To date, only a few MOFs containing bptc ligand have been characterized. Examples

(14) (a) Sheldrick, G. M. *SHELXS 97, Program for Crystal Structure Solution;* University of Göttingen: Göttingen, Germany, 1997. (b) Sheldrick, G. M. *SHELXL 97, Program for Crystal Structure Refinement;* University of Göttingen: Göttingen, Germany, 1997.

Table 2. Selected Bond Lengths (angstroms) and Angles (deg) for **1** and **2**[a]

1			
Zn(1)−O(1)	1.922(14)	Zn(1)−N(1)	2.058(5)
Zn(1)−O(4)#1	1.984(6)	Zn(1)−O(2)	2.285(14)
Zn(1)−N(2)	2.037(6)		
O(1)−Zn(1)−O(4)#1	128.5(5)	N(2)−Zn(1)−N(1)	102.1(2)
O(1)−Zn(1)−N(2)	85.9(4)	O(1)−Zn(1)−O(2)	54.8(4)
O(4)#1−Zn(1)−N(2)	105.6(2)	O(4)#1−Zn(1)−O(2)	96.8(4)
O(1)−Zn(1)−N(1)	108.3(4)	N(2)−Zn(1)−O(2)	140.4(3)
O(4)#1−Zn(1)−N(1)	117.3(3)	N(1)−Zn(1)−O(2)	95.9(4)
2			
Cd(1)−N(1)	2.2617(16)	Cd(1)−OW1	2.3502(15)
Cd(1)−O(2)	2.2783(16)	Cd(1)−O(1)	2.4692(15)
Cd(1)−O(4)#1	2.2824(16)	Cd(1)−O(3)#2	2.5368(17)
OW1···OW2	2.713(39)	OW2···O4	2.851(10)
N(1)−Cd(1)−O(2)	153.49(6)	O(4)#1−Cd(1)−O(1)	136.52(6)
N(1)−Cd(1)−O(4)#1	119.41(6)	OW1−Cd(1)−O(1)	79.58(6)
O(2)−Cd(1)−O(4)#1	86.90(6)	N(1)−Cd(1)−O(3)#2	77.83(6)
N(1)−Cd(1)−OW1	87.51(6)	O(2)−Cd(1)−O(3)#2	88.73(6)
O(2)−Cd(1)−OW1	98.08(6)	O(4)#1−Cd(1)−O(3)#2	114.24(6)
O(4)#1−Cd(1)−OW1	86.51(6)	OW1−Cd(1)−O(3)#2	158.58(5)
N(1)−Cd(1)−O(1)	101.04(6)	O(1)−Cd(1)−O(3)#2	87.91(6)
O(2)−Cd(1)−O(1)	55.21(5)		

[a] Symmetry transformations used to generate equivalent atoms for 1: #1 $x, -y+1, z+1/2$; for 2: #1 $-x, y-1, -z+3/2$; #2 $x, -y+2, z-1/2$.

of such compounds include the 1D chain complexes $\{[Zn(H_2O)_6][Zn(bptc)H_2O]\cdot 4H_2O\}_n$,[19a] $[M_2(cfH)_2(bptc)(H_2O)_2]\cdot 8H_2O$ (M = Mn and Cd),[12e] the 2D layer complexes $[Cd_2Cu(Hbptc)_2(\mu_2\text{-}4,4'\text{-bpy})_2(4,4'\text{-bpy})_2(H_2O)_2]_n$,[19b] $[M_2(bptc)(bpy)_{0.5}(H_2O)_5]\cdot 0.5bpy$ (M = Mn, Mg, and Co),[9f] $[Zn_2(cfH)_2(bptc)]\cdot 4H_2O$,[12h] and the 3D pillared-layer complexes $[M_3(Hbptc)_2(bpy)_3(H_2O)_4]\cdot 2H_2O$ (M = Fe and Ni), $[Cu_2(bptc)(bpy)_2]$, $[Co_2(bptc)(bpy)(H_2O)]\cdot 0.5bpy$, $[Cd_2(bptc)(bpy)(H_2O)_2]\cdot H_2O$, $[Mn_2(bptc)(bpy)_{1.5}(H_2O)_3]$,[9f] $[Co_3(Hbptc)_2(\mu_2\text{-}4,4'\text{-bpy})_3(H_2O)_4]_n\cdot 2nH_2O$,[19b] and $[Co_2(bptc)(pyz)(H_2O)_4]\cdot H_2O$.[19c] The coordination modes of bptc in structurally characterized coordination polymers observed up to now are summarized in Scheme S1. As can be seen, the bptc ligand possesses three possible conformations and multiple bridging moieties, which may lead to a variety of coordination modes with metal centers and provide abundant structural motifs, thereby offering new opportunities to construct uncommon types of entangled frames. (iv) The coordination chemistry of the sdba ligand has not been previously investigated.

Descriptions of Crystal Structures. Single-crystal X-ray diffraction analysis reveals that **1** is a binodal four-connected 3D self-penetrating network with an unprecedented topology whose structure contains two types of helices and three types of molecular braids. The crystallographically independent Zn atom adopts a distorted square-pyramidal geometry (Figure 5a), being coordinated with two nitrogen atoms from two bpy ligands and three oxygen atoms from two bptc ligands. The bptc ligand adopts a hexadentate chelating and bridging coordination mode; two carboxylate groups chelate with two Zn^{II} ions bidentately, whereas the other two adopt a monodentate coordination mode connecting two other metal ions (Scheme S1(*l*)). This coordination mode has not been observed in other metal-bptc complexes.[9f,12e,h,19] On the basis of this connection mode, the Zn atoms are bridged by bptc ligands to form a 1D tubular channel (with dimensions of

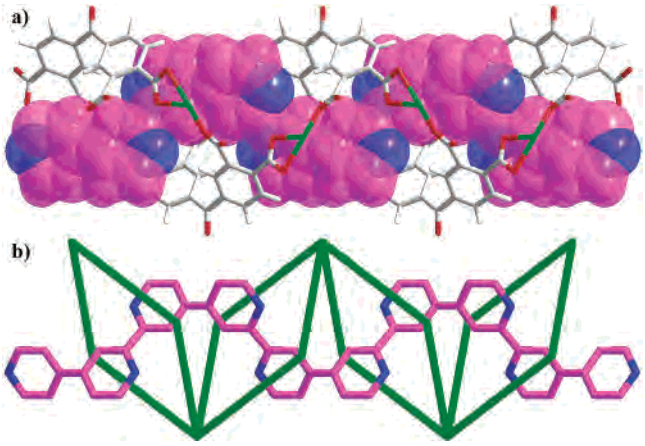

Figure 1. (a) View of the 1D tubular channel in **1**, highlighting the poly(4,4′-bpy) chain is well matched with the channel. (b) A schematic illustration of the unusual poly(pseudo-rotaxane) array in **1**.

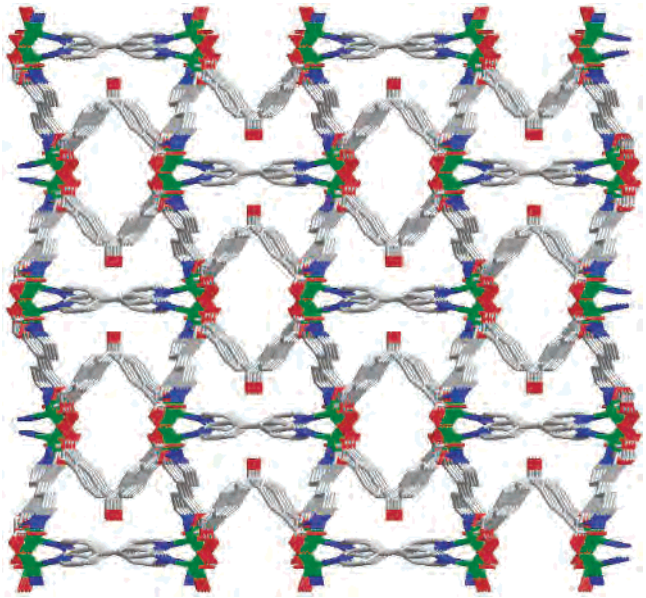

Figure 2. Perspective view of the 3D open framework of **1**.

9.79×11.68 Å^2) of composition $[Zn_2(bpdc)]$ running along the *c* axis (Figures 1 and S1). As depicted in Figure 2, each tubular channel is connected to six others through bpy ligands to generate a novel 3D framework (Figure S3), which can also be considered as being constructed from 2D neutral layers of composition $[Zn_2(bpdc)(bpy)]$ (Figure S2) linked by bpy ligands. It is surprising that the in situ hydrothermal synthesis of poly(4,4′-bpy) by dehydrogenative polymerization of uncoordinated 4,4′-bpy molecules occurs in the tubular channels of **1** (Figure 1). The in situ dehydrogenative coupling of bipyridine-like ligands under hydrothermal conditions has been previously reported by us and others.[15a,b] As evidenced in a recent review,[16] hydrothermal reactions, compared with routine synthetic methods, create more chance for in situ ligand synthesis owing to their relatively critical

(15) (a) Liu, C. M.; Gao, S.; Kou, H.-Z. *Chem. Commun.* **2001**, 1670. (b) Xiao, D. R.; Hou, Y.; Wang, E. B.; Lou, J.; Li, Y. G.; Xu, L.; Hu, C. W. *Inorg. Chem. Commun.* **2004**, *7*, 437. (c) Zhang, J.-P.; Lin, Y.-Y.; Huang, X.-C.; Chen, X.-M. *J. Am. Chem. Soc.* **2005**, *127*, 5495.
(16) Zhang, X.-M. *Coord. Chem. Rev.* **2005**, *249*, 1201 and references therein.

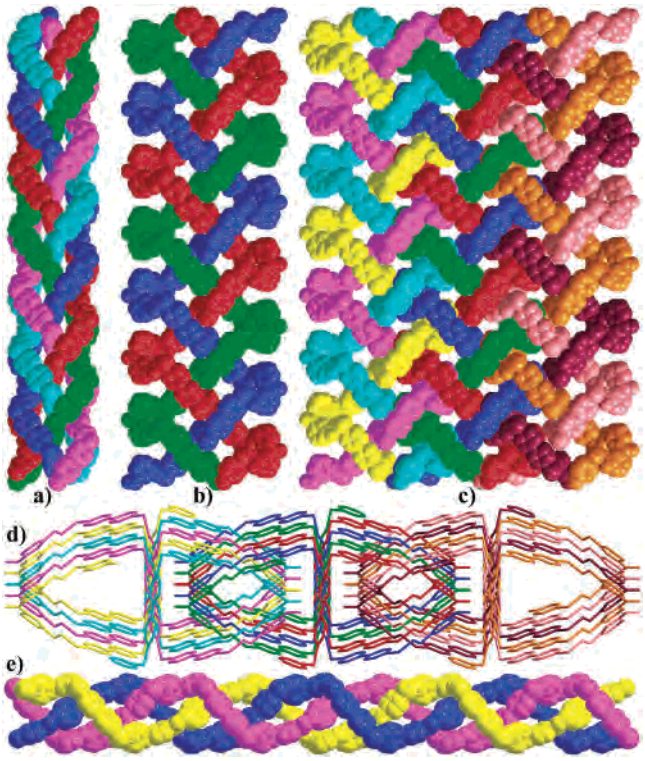

Figure 3. Space-filling views of the quadruple-stranded molecular braid. (a) The first type of triple-stranded molecular braid, (b) the 9-fold interwoven meso helix, (c) and the second type of triple-stranded molecular braid (e) in **1**. (d) Side view of the 9-fold interwoven meso helix along the *c* axis.

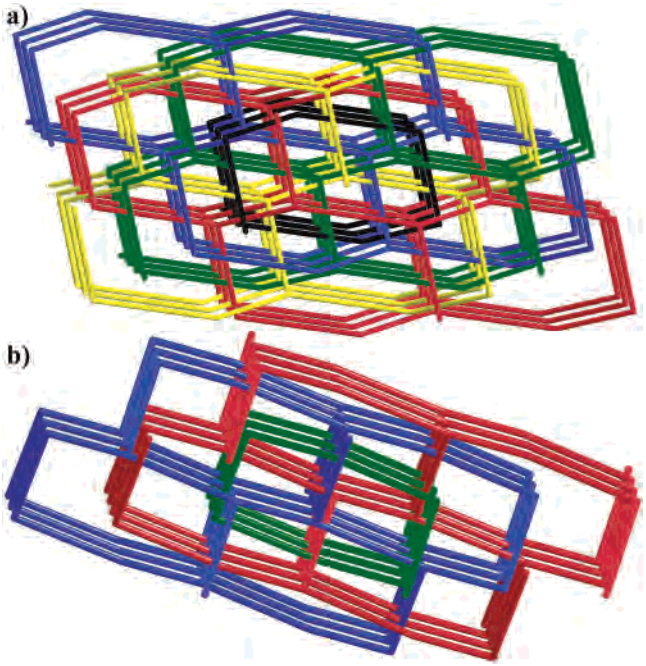

Figure 4. Schematic views of the entangled motifs originated from 17 interwoven A-type helices (a) and 9 interwoven B-type helices (b).

reaction conditions. Therefore, the high temperature and pressure and long-time reactions, as well as the presence of Zn^{II} ions, may facilitate the in situ synthesis of poly(4,4′-bpy) (Scheme S4). It is worth noting that the MOFs, which are based on in situ generated ligands, especially on ligands unreachable by conventional methods, are of great interest in both coordination and organic chemistry because they

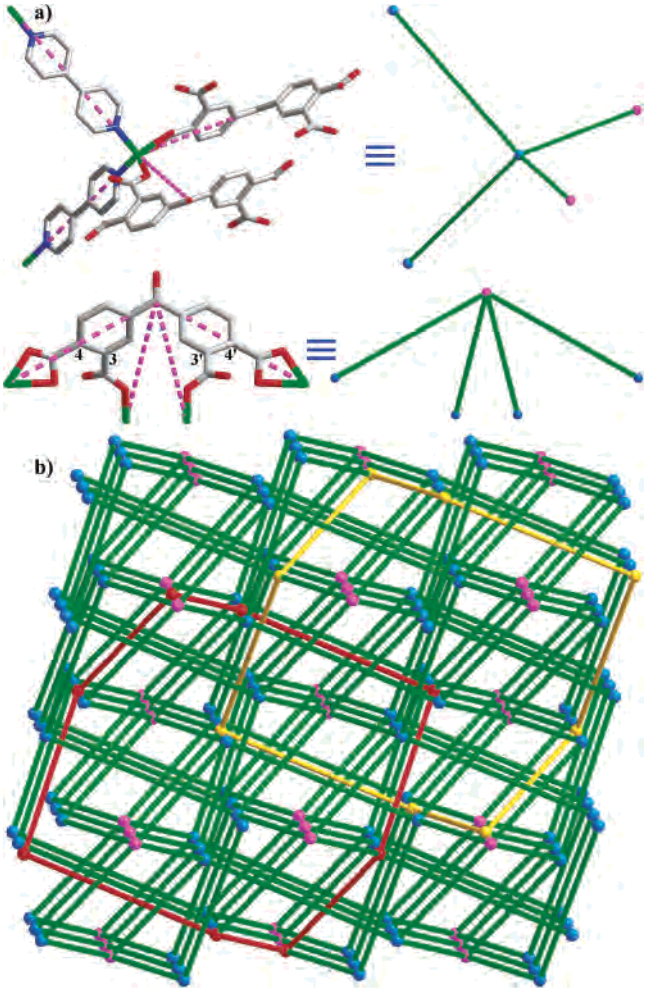

Figure 5. (a) Perspective views of the four-connected (Zn atom and bptc ligand) nodes in **1**. Purple dashed lines illustrate the four-connected circumstances of Zn and bptc, respectively. (b) Schematic representation of the binodal four-connected self-penetrating 3D net of $(4.6^2.8^3)_2(4^2.6^2.8^2)$ topology (color code: Zn light-blue, C purple). The self-penetrating shortest circuits are highlighted.

facilitate new organic reactions and stabilize unstable species.[15,16] Furthermore, a careful examination of the crystal structure of **1** reveals that the poly(4,4′-bpy) chain and tubular channel are well matched with each other (Figure 1a), implying that a molecular recognition between them occurs through very strong $\pi-\pi$ stacking interactions (interplanar distance 3.17 Å). We believed that the very strong $\pi-\pi$ stacking interactions play an important role in stabilizing the poly(4,4′-bpy) chains and tubular channels. Moreover, as illustrated in Figure 1b, the poly(4,4′-bpy) chain threads into the large rings of the tubular channel, thus resulting in an unusual poly(pseudo-rotaxane) array.

The most fascinating and peculiar structural feature of **1** is that a quintuple-stranded molecular braid and two types of triple-stranded molecular braids (Figure 3) coexist in the 3D network of **1**. This case is unprecedented even though two elegant coordination networks containing triple-stranded molecular braids have previously been reported.[10] As depicted in Figure 3a, the Zn atoms are bridged by the bpy and benzophenone-4,4′-dicarboxylate groups of bptc ligands to form the quintuple-stranded molecular braid running along the crystallographic *c* axis with a pitch of 64.015 Å (Figure

S4a). To the best of our knowledge, **1** represents the first and only example of a polymeric coordination network containing a quintuple-stranded molecular braid. The unusual quintuple-stranded molecular braid represents the highest-stranded molecular braid known in the field of coordination polymers and inorganic compounds. The first type of triple-stranded molecular braid (Figure 3b) is constructed by bpy and benzophenone-3,3′-dicarboxylate groups of bptc ligands bridged between the Zn centers, which is extended along the *c* axis with a period of 38.409 Å (Figures S4b and S5). Each triple-stranded molecular braid further intertwines with two neighboring triple-stranded molecular braids to give an unprecedented 9-fold interwoven meso helix (Figure 3c,d). To our knowledge, the 9-fold meso helix exhibits the highest degree of entanglement ever found in a self-penetrating system.[6] The second type of triple-stranded molecular braid (Figure 3e), which runs along the [1 0 $\bar{1}$] direction with a pitch of 73.517 Å, is formed by bpy, benzophenone-3,4′-dicarboxylate groups, and benzophenone-4,4′-dicarboxylate groups of bptc ligands bridging the Zn atoms (Figure S4c). In addition, **1** also contains a single-stranded meso helix (Figure S6) that is built from bpy and benzophenone-3,3′-dicarboxylate groups of bptc ligands that bridge between the Zn centers running along the [1 0 $\bar{1}$] direction with a pitch of 24.506 Å. Up to now, the meso helical molecules are still quite uncommon, and only a few meso helical coordination polymers have been characterized.[10−11]

Apart from the intrinsic interest of three types of molecular braids, another notable feature of **1** is the existence of two types of helical chains running along a crystallographic 2_1 axis in the *b* direction with a pitch of 16.768 Å. The first type of helix (code A) is built from bpy and benzophenone-4,4′-dicarboxylate groups of bptc ligands that bridge between the Zn centers (Figure S7), whereas the second type of helix (code B) is formed by bpy and benzophenone-3,3′-dicarboxylate groups of bptc ligands bridging the Zn atoms (Figure S8). The helical tube formed by the A-type helix is larger than that observed in the B-type helix. Most exciting, however, is the fact that each A-type helix is further intertwined with 16 A-type helices (8 same handedness and 8 opposite) in all directions to produce an exceptional entangled motif originated from 17 interwoven helices (Figures 4 and S9). Similarly, an entangled array originating from 9 interwoven B-type helices (Figures 4 and S10) is also formed in **1**. As far as we know, such entangled motifs originating from *n*-fold interwoven helices are still very rare in the system of metal-organic complexes. Only two known entangled arrays containing 9-fold helices were reported by our group very recently,[12a,d] in which 9 independent helices interweave in a manner similar to that observed in a rather remarkable example reported by Lin's group.[9a]

From the topological point of view,[1f] the 3D structure of **1** can be simplified to a unique binodal four-connected net with an unprecedented $(4.6^2.8^3)_2(4^2.6^2.8^2)$ topology (Figure 5b).[20] In this simplification, the Zn atom acts as one kind of the four-connected node $(4.6^2.8^3)$, and the C17 atom of the bptc ligand acts as the other $(4^2.6^2.8^2)$ (Figure 5a). We note that some of the 8-membered shortest rings are catenated

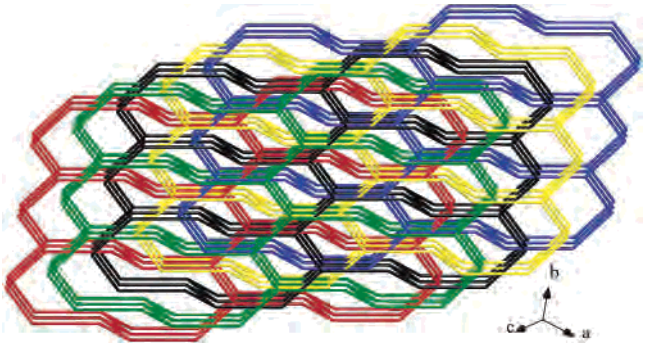

Figure 6. Schematic illustration of the 5-fold interpenetrating (10,3)-b frame isolated by removing 3,3′-carboxylate groups from **1**.

by other equivalent 8-membered rings within the same network (Figures 5b and S13), illustrating that this net is an unusual self-penetrating one, noting that only a limited number of self-penetrated nets have been reported to date.[6] A better insight into the nature of this intricate architecture can be achieved if one can imagine removing one of the two types of carboxylate groups of bptc ligands at a time (Figure 5a).[6g] On removing the 3,3′-carboxylate groups, the remainder is an intriguing 5-fold interpenetrating 3D three-connected framework with (10,3)-b topology (Figures 6 and S14).[20] To our knowledge, the 5-fold interpenetrating (10,3)-b net has not been identified until now.[5b] On the other hand, elimination of 4,4′-carboxylate groups leaves a 3-fold interpenetrating (10,3)-b subnet (Figures S16 and S17). Generally, if *n*-fold interpenetrating networks are joined together through extra connections, a single self-penetrating net with higher connectivity will be obtained.[2a] Therefore, the overall framework of **1** is clearly a self-penetrating net and can be considered as derived from 5-fold or 3-fold interpenetrating (10,3)-b subnets that are crosslinked by extra connections (Figures S18−S21).

When dicarboxylate ligand sdba is used instead of bptc, an uncommon 2D self-penetrating network with an unprecedented topology is produced. The crystallographically independent Cd atom is coordinated by one nitrogen atom from a bpy ligand, four oxygen atoms from one chelating and two μ_2-bridging carboxylate groups coming from three sdba ligands, and one aqua ligand to furnish a distorted octahedral geometry. Two Cd atoms are bridged by a pair of μ_2-carboxylate ends to give dinuclear units that are farther extended by sdba bridging ligands into a 2D layer that exhibits very large octagonal windows (19.0 × 20.6 Å, Figure S22a). When the Cd and S atoms of sdba ligands are regarded as nodes, the 2D layer can be simplified to a three-connected net with (4.8^2) topology (Figure S22b). The 2D layers are highly undulated as a consequence of the bent geometry of the sdba ligands and the twisting of its phenyl rings. The large octagonal windows and the corrugation of the single sheets allow one identical (4.8^2) network to interpenetrate the octagonal windows in a parallel mode, thus giving a 2-fold interpenetrating array containing double-stranded helices (Figure 7c). Interpenetration of layers with (4.8^2) topology is rare if compared with layers that show the more common (4^4) or (6^3) topologies, and only few examples are known that include sheets that are interpen-

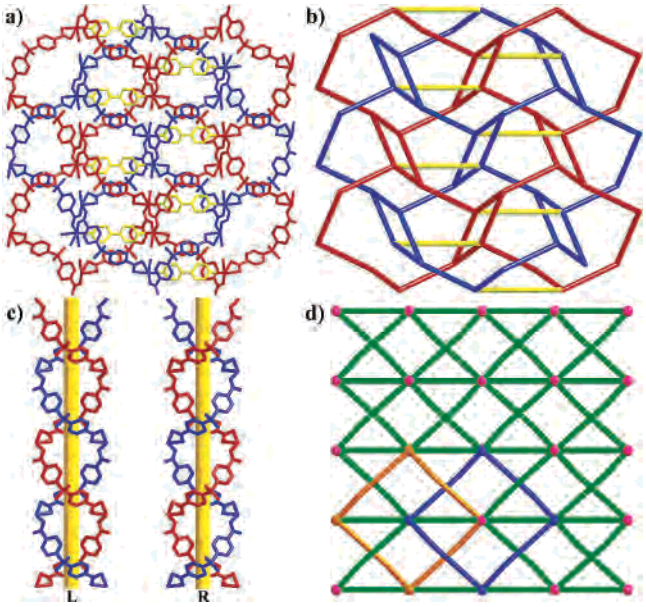

Figure 7. (a) Perspective and (b) schematic views of the (3,4)-connected self-penetrating 2D net of $(4.6.8)(4.6^2.8^3)$ topology of **2**. (c) Perspective view of the double-stranded helices in **2**. (d) A schematic representation of the six-connected self-penetrating 2D net of $4^{13}.6^2$ topology of **2**. The self-penetrating shortest circuits are highlighted.

etrated in a parallel 2-fold and 3-fold manner.[5] More interestingly, the bpy ligands, acting as the extra bridging molecules, connect two identical (4.8^2) networks together to generate a unique (3,4)-connected 2D self-penetrating network (Figure 7a,b) with an unprecedented $(4.6.8)(4.6^2.8^3)$ topology (the first symbol for S atom of sdba ligand, the second one for Cd atom).[20] Catenations of the eight-membered shortest circuits by other eight-membered shortest circuits are observed in **2**. So far, the 2D self-penetrating networks are extremely rare, as evidenced in a recent review.[2a] To our knowledge, only two 2D self-penetrated networks have been reported up to now.[17]

Similar to **1**, further insight into the nature of the topologically complex layer can be obtained if one can imagine removing one of the four types of links of different lengths at a time (Figure S23a). On removing type I (11.525 Å), the remainder is the 2-fold interpenetrating (4.8^2) network described above. However, elimination of type II (7.595 Å, corresponding to the removal of the longest Cd−O bond) leaves a 2D three-connected frame with (6^3) topology, exhibiting an unusual 4-fold entanglement (Figure S24a). At first glance, the subnet seems like a parallel 4-fold interpenetrating (6^3) network. However, a careful examination shows that the entanglement consists of two sets of interpenetrating chiral layers, one left-handed (yellow and red) and the other right-handed (blue and green). Strikingly, the adjacent layers belonging to different sets are neither interpenetrated nor catenated (Figure S24) but are entangled via pseudo-Borromean links.[2b] This becomes apparent when considering three six-membered rings (Figure 8a) from three

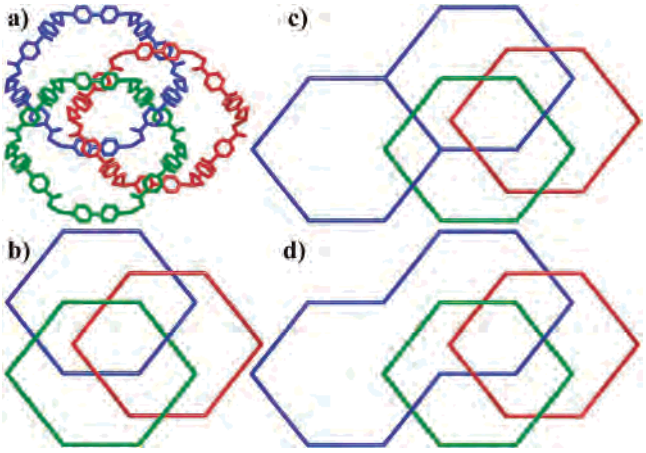

Figure 8. (a) Perspective and (b) schematic views of the pseudo-Borromean links of three 6-membered rings in **2**. The elemental entanglement between the two sets of non-catenated layers is equivalent to the nontrivial linkage (c), which can be transformed into Borromean links (d).

different adjacent layers that are entangled as the three pseudo-Borromean rings (Figure 8b). The nature of the entanglement between the two sets of non-catenated layers can be clearly seen in Figure 8c,d: the catenation of the blue and green rings prevents the disentanglement of the (non-catenated) red one (c); this entanglement can also be transformed into Borromean links (d).[2a,b] This kind of entanglement is still quite uncommon,[2b] and a remarkable example is $[Ag_2(H_2L)_3](NO_3)_2$ (H2L = N,N′-bis(salicylidene)-1,4-di-aminobutane),[18]in which the overall structure can be described as a four-connected self-penetrating net. However, if the Ag···Ag interactions are ignored, the structure is a 3D Borromean array.[2b] Another noteworthy aspect of the 2D self-penetrating net in **2** is the fact that the (3,4)-connected net can also be simplified to a six-connected self-penetrating net with an unprecedented ($4^{13}.6^2$) topology by considering the dinuclear units as six-connected nodes (Figures 7d and S23b,d). The self-catenation of the four-membered shortest rings by other four-membered rings is illustrated in Figure 7d.

In the packing arrangement of **2**, the adjacent layers are interconnected by strong hydrogen bonding interactions (OW1···OW2 = 2.713 Å and OW2···O4 = 2.851 Å) to generate a 3D supramolecular network (Figure S26a). When these hydrogen bonds are taken into account,[2a,12b] the resulting structure can be simplified to a (3,5)-connected 3D self-penetrating network with an unprecedented (4.6.8)-$(4.6^2.7^5.8^2)$ topology (Figures 9a and S27a,b). The catenated eight-membered shortest rings are observed in Figure 9a. It is noteworthy here to mention that the 3D self-penetrating network can also be considered as constructed from the unusual 4-fold (2 + 2) interpenetrating diamond nets (Figure

(17) (a) Carlucci, L.; Ciani, G.; Macchi, P.; Proserpio, D. M.; Rizzato, S. *Chem.—Eur. J.* **1999**, *5*, 237. (b) Plater, M. J.; Foreman, M. R. J. St.; Gelbrich, T.; Hursthouse, M. B. *J. Chem. Soc., Dalton Trans.* **2000**, 1995.

(18) Tong, M. L.; Chen, X.-M.; Ye, B.-H.; Ji, L.-N. *Angew. Chem., Int. Ed.* **1999**, *38*, 2237.

(19) (a) Yang, Y.-Y.; Szeto, L.; Wong, W.-T. *Appl. Organomet. Chem.* **2003**, *17*, 958. (b) Zhang, J.; Li, Z.-J.; Kang, Y.; Cheng, J.-K.; Yao, Y.-G. *Inorg. Chem.* **2004**, *43*, 8085. (c) Zhang, J.; Li, Z.-J.; Cheng, J.-K.; Kang, Y.; Qin, Y.-Y.; Yao, Y.-G. *New J. Chem.* **2005**, *29*, 421.

(20) Structure analysis and reduction performed using the DIAMOND program. Brandenburg K.; Putz GbR, H. *DIAMOND - Crystal and Molecular Structure Visualization - Demonstration*, version 3.0; Crystal Impact: Bonn, Germany, 2004.

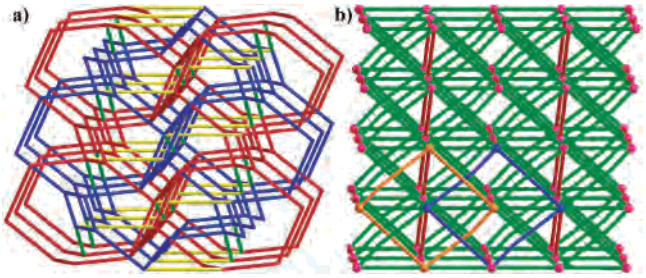

Figure 9. (a) Schematic view of the (3,5)-connected self-penetrating 3D net of $(4.6.8)(4.6^2.7^5.8^2)$ topology of **2**. (b) Schematic representation of the eight-connected self-penetrating 3D net of $4^{21}.6^7$ topology of **2**. The self-penetrating shortest circuits are highlighted.

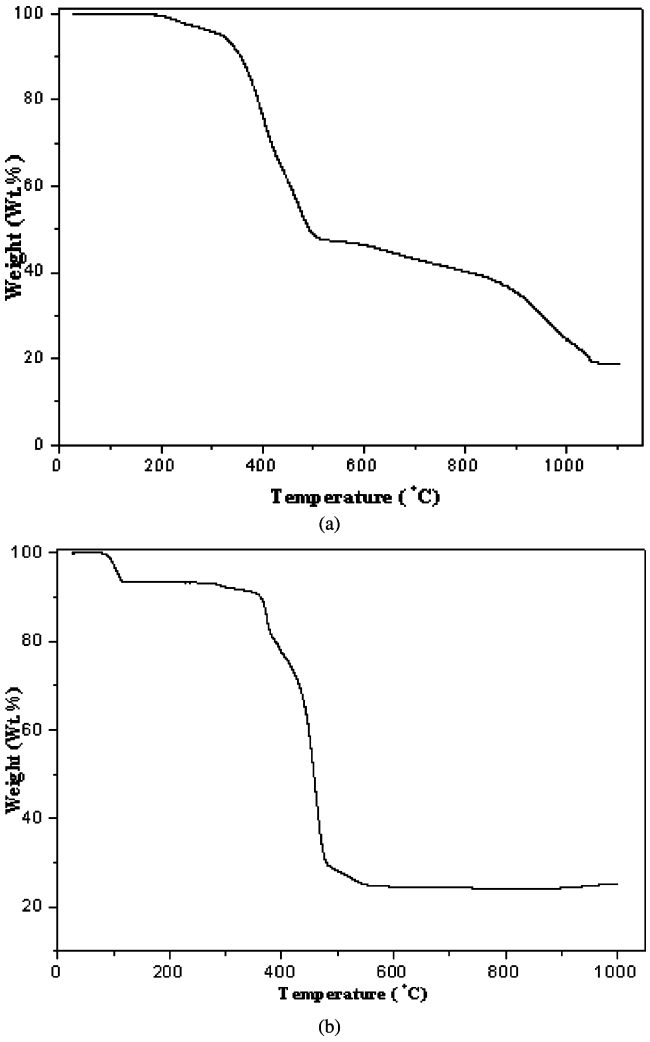

Figure 10. TG curves of **1** (a) and **2** (b), respectively.

S28b),[13a] which are crosslinked by the extra connections (namely type II, Figure S29). More interestingly, if the $[Cd_2(CO_2)_2]$ dinuclear unit is regarded as an eight-connected node (Figure S27c,d), the 3D structure of **2** can also be rationalized as an eight-connected self-penetrating net symbolized as $(4^{21}.6^7)$ (Figure 9b), which is unprecedented. The eight-connected self-penetrating coordination polymers are, at present, rare. Only two eight-connected self-penetrating coordination networks were reported by our group very recently,[12f,g] in which the topologies $(4^{24}.5.6^3$ and $4^{20}.6^8)$ are significantly different from that of **2**. Therefore, to our knowledge, **2** also represents the highest connected topology at present known for self-penetrating systems.

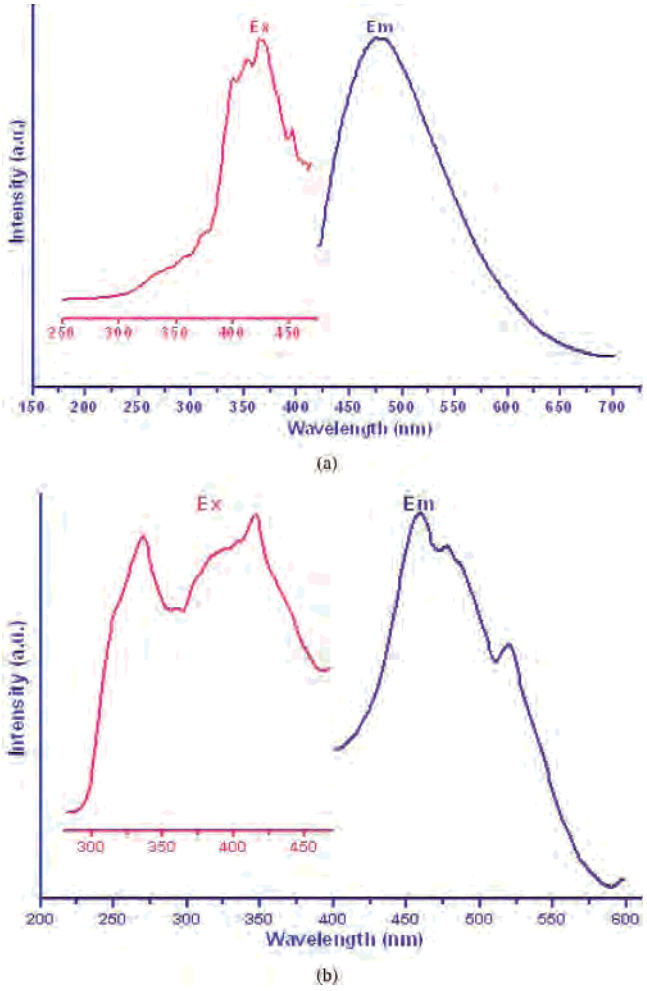

Figure 11. Solid-state emission spectra of complexes at room temperature: (a) **1**, (b) **2**.

Thermal Stability Analysis. To examine the thermal stability of the two compounds, thermal gravimetric (TG) analyses were carried out for **1** and **2** (Figure 10). The TG curve of **1** exhibits four weight loss stages in the temperature ranges of 180−295 (3.95%), 295−520 (48.40%), 520−820 (8.01%), and 820−1060 °C (20.65%) (Figure 10a), corresponding to the release of water molecules, poly(4,4′-bpy), bpy, and bptc ligands. The residue is ZnO. The whole weight loss (81.01%) is in good agreement with the calculated value (81.33%).

The TG curve of **2** is shown in Figure 10b. It gives a total weight loss of 75.04% in the range of 75−565 °C, which agrees with the calculated value of 75.81%. The first weight loss is 6.43% in the temperature range of 75−120 °C, which corresponds to the loss of all non-coordinated and coordinated water molecules (calcd 6.79%), and then the sample keeps relatively stable in the temperature range of 120−270 °C, probably suggesting the formation of a stable phase formulated as $[Cd_2(sdba)_2(bpy)]$. The second weight loss is 1.77% at 270−340 °C; the third step is 13.90% from 340 to 400 °C, and the last step is 52.94% in the temperature range of 400−565 °C, all assigned to the decomposition of bpy

and sdba ligands (calcd 69.02%). The remaining weight (24.96%) indicates that the final residue was CdO (calcd 24.19%).

Photoluminescence Properties. Taking the luminescent properties of d^{10} metal complexes into account, the luminescence of **1** and **2** was investigated. It can be observed that intense blue fluorescent emissions occur at 475 nm (Figure 11a, λ_{ex} = 398 nm) for **1** and 459 nm (Figure 11b, λ_{ex}=320 nm) for **2**. To understand the nature of the emission band, the photoluminescence properties of H_4bptc and H_2sdba ligand were analyzed. Two weak emissions at 476 and 329 nm were observed for free H_4bptc and H_2sdba ligands, respectively (Figure S31). Therefore, the emission of **1** may be assigned to the intraligand fluorescent emission, whereas the emission of **2** may be attributable to ligand-to-metal charge transfer.[12] The enhancement of luminescence may be attributed to ligand chelation to the metal center, which effectively increases the rigidity of the ligand and reduces the loss of energy by radiationless decay. These observations indicate that **1** and **2** may be candidates for potential photoactive materials.

Conclusions

In summary, we have prepared and characterized two unprecedented self-penetrating coordination networks with uncommon entangled motifs, such as the quintuple-stranded molecular braid, the 9-fold meso helices, and the 17-fold interwoven helices, which fill the lacunas in the realm of entanglement. The isolation of both compounds not only provides unprecedented examples of chemical topology but also confirms the aesthetic diversity of coordinative network chemistry. Topological analyses of two complexes have revealed the relationships between the self-penetrating nets and related interpenetrating nets, which may provide new insights into the analysis and design of self-penetrating networks.

Acknowledgment. The authors thank the National Natural Science Foundation of China (grant no. 20371011) for financial support.

Supporting Information Available: X-ray crystallographic files for **1** and **2** in CIF format and additional plots of the structures. This material is available free of charge via the Internet at http://pubs.acs.org.

IC070054A